Analysis of monotonic greening and browning trends from global NDVI time-series

de Jong, Rogier ; de Bruin, S ; de Wit, A ; Schaepman, Michael E ; Dent, D L

Abstract: Remotely sensed vegetation indices are widely used to detect greening and browning trends; especially the global coverage of time-series normalized difference vegetation index (NDVI) data which are available from 1981. Seasonality and serial auto-correlation in the data have previously been dealt with by integrating the data to annual values; as an alternative to reducing the temporal resolution, we apply harmonic analyses and non-parametric trend tests to the GIMMS NDVI dataset (1981-2006). Using the complete dataset, greening and browning trends were analyzed using a linear model corrected for seasonality by subtracting the seasonal component, and a seasonal non-parametric model. In a third approach, phenological shift and variation in length of growing season were accounted for by analyzing the time-series using vegetation development stages rather than calendar days. Results differed substantially between the models, even though the input data were the same. Prominent regional greening trends identified by several other studies were confirmed but the models were inconsistent in areas with weak trends. The linear model using data corrected for seasonality showed similar trend slopes to those described in previous work using linear models on yearly mean values. The non-parametric models demonstrated the significant influence of variations in phenology; accounting for these variations should yield more robust trend analyses and better understanding of vegetation trends.

DOI: https://doi.org/10.1016/j.rse.2010.10.011

Elsevier Editorial System(tm) for Remote Sensing of Environment
Manuscript Draft

Manuscript Number:

Title: Analysis of monotonic greening and browning trends from global NDVI time-series

Article Type: Full length article

Keywords: Global vegetation trends; Phenology; Harmonic analysis; GIMMS NDVI; seasonal Mann-Kendall

Corresponding Author: Mr. Rogier de Jong,

Corresponding Author's Institution: Wagenigen University

First Author: Rogier de Jong, MSc

Order of Authors: Rogier de Jong, MSc; Sytze de Bruin, dr; Allard de Wit, dr; Michael E Schaepman, prof dr; David L Dent, dr

Analysis of monotonic greening and browning trends from global NDVI time-series

Rogier de Jong [a,b,*], Sytze de Bruin [a], Allard de Wit [c], Michael E. Schaepman [d,a], David L. Dent [e]

a Centre for Geo-Information, Wageningen University, The Netherlands

b ISRIC - World Soil Information, Wageningen, The Netherlands

c Alterra, Wageningen, The Netherlands

d Remote Sensing Laboratories, University of Zurich, Switzerland

e Merchants of Light Ltd, Norwich, England

* corresponding author.

Postal address: P.O. Box 47, 6700 AA Wageningen, The Netherlands. *E-mail address:* Rogier.deJong@wur.nl. *Phone:* +31 317483734. *Fax:* +31 317 419000.

Abstract

Remotely sensed vegetation indices are widely used indicators of land degradation; in particular global coverage of time-series of normalized difference vegetation index (NDVI) data which are available from 1981. Seasonality and serial auto-correlation in the data have previously been dealt with by reducing the temporal resolution to annual values; here, we apply harmonic analyses and non-parametric trend tests to the GIMMS NDVI dataset (1981-2006) as an alternative to reducing the temporal resolution. The full dataset was analyzed for greening and browning trends using a linear model, corrected for seasonality by subtracting the long-term seasonal component, and a seasonal non-parametric model. In a third approach, phenological shift and variation in length of growing season were taken into account by analyzing the time-series using vegetation development stages rather than calendar days. Results differed

substantially between the models, even though the input data were the same. Prominent regional greening trends identified by several other studies were confirmed but, in areas with weak trends, the models were inconsistent. The linear model using de-seasonalized data showed similar trend slopes to that described in previous work using linear models on yearly mean values. The non-parametric models demonstrated the significant influence of variations in phenology; accounting for these variations should yield more robust trend analyses and better understanding of NDVI trends.

Keywords: Global vegetation trends; Phenology; Harmonic analysis; GIMMS NDVI; seasonal Mann-Kendall

1. Introduction

Vegetation, as the main component of the terrestrial biosphere, is a crucial element in the climate system (Foley et al., 2000) and there is high confidence that recent global warming is strongly affecting the terrestrial biosphere (IPCC, 2007). Vegetation status is commonly used in assessments of productivity of natural and agricultural lands (Cai and Sharma, 2010; Sims et al., 2008; Yu et al., 2009) and a declining trend is considered to be indicative of land degradation (Metternicht et al., 2010; Zika and Erb, 2009). Land degradation is a global environmental and socio-economic issue (UNEP, 2007) but its extent and severity is only roughly known and there is no agreement on its definition – or on appropriate ways to monitor the situation (de Jong et al., 2010); global assessments have been mainly confined to descriptive mapping. The only way to quantify vegetation variability consistently at a global scale is by use of satellite remote sensing using long time-series of images with a regular acquisition interval (Justice et al., 1985). Normalized Difference Vegetation Index (NDVI), based on red and near-infrared reflectance (Tucker, 1979), has been proven to be a valid proxy for greening or browning trends – which

53 may be interpreted as change in ecosystem function and productivity (Alcaraz-Segura et al.,
54 2009; Bai et al., 2008). It has become the most-used product derived from National
55 Oceanographic and Atmospheric Administration (NOAA) Advanced Very High Resolution
56 Radiometer (AVHRR) data (Cracknell, 2001). However, it is difficult to attribute cause and
57 effect to vegetation trends because various factors, including climatic cycles, drive variations in
58 vegetation productivity.

59 Trends and inter-annual variability in vegetation phenology affect the exchange of carbon,
60 water and energy exchange between the vegetation and the atmosphere (Baldocchi et al., 2001).
61 Satellite observations since the early 1980s give high confidence that there has been a widespread
62 trend towards earlier onset of greening and longer thermal growing seasons in many regions,
63 especially in the Northern Hemisphere (IPCC, 2007; Karlsen et al., 2007; Myneni et al., 1997;
64 Tucker et al., 2001). This is in line with the increase in net primary production (NPP) suggested
65 by modeling (Nemani et al., 2003) and is confirmed by field observations (Barford et al., 2001;
66 Menzel et al., 2006). Longer and warmer growing seasons increase evapo-transpiration and
67 drought stress (Barber et al., 2000; Zhang et al., 2009), wildfire incidence (Westerling et al.,
68 2006) and intensity of carbon sequestration (Goulden et al., 1996; White et al., 1999), all of
69 which are likely to be a part of land degradation.

70 Most analyses have used a linear model with annual cumulative NDVI to estimate trends.
71 However, it is not always clear whether the slope differs significantly from zero (de Beurs and
72 Henebry, 2004) or what may be the effect of averaging by calendar year in the southern
73 hemisphere (Wessels, 2009). Also, linear regression of NDVI time series needs to be used with
74 care because any auto-correlation within the dataset will violate some model assumptions (Beck
75 et al., 2006; de Beurs and Henebry, 2004; McBride et al., 1994). If trends are to be distinguished

from cyclical variation, seasonality must be compensated for or removed (Hussian et al., 2005); alternatively, a seasonal Mann-Kendall trend test may be applied (de Beurs and Henebry, 2004).

Here, we investigate monotonic trends – so trends which preserve their increasing or decreasing order throughout the time-series. We examine differences between previously-published methods and suggested improvements using the Global Inventory Modeling and Mapping Studies (GIMMS) NDVI dataset (1981-2006) without reducing its temporal resolution in the cases of (1) a linear model applied to *de-seasonalized* data (i.e. NDVI residuals after the seasonal component has been removed); (2) a non-parametric model applied to the original NDVI data and (3) a non-parametric model applied to data in which phenological cycles are adjusted to the same start and length of growing season. Long-term and annual harmonic analyses were used to filter cloudiness and seasonality, and to derive phenological measures that take account of inter-annual variations in phenology. Although satellite-observed phenology, often referred to as land-surface phenology (LSP), is not identical to plant phenology, it is considered to be related (Doktor et al., 2009; Liang and Schwartz, 2009; White et al., 2009). We account for variations in LSP by analyzing trends in productivity based on vegetation development stages rather than on calendar days.

2. Materials and Methods

The methods used in this study include pre-processing of the NDVI data using harmonic analysis; removing seasonality from data by subtracting short-term (yearly) harmonic fits from the long-term (26 years) fit; and application of linear and non-parametric models, summarizing the outputs by biome.

2.1. The GIMMS dataset

98 We used GIMMS version G (Tucker et al., 2004), consisting of 26 years of NDVI data from
99 1981 through 2006, summarized fortnightly at 8km resolution. The fortnightly 8-km time-series
100 was derived from daily 4km global area coverage (GAC) data from a suite of NOAA satellites
101 (Tucker et al., 2005), applying the maximum-value-composite (MVC) technique to remove bias
102 caused by atmospheric conditions (Holben, 1986). However, it is not an atmospheric-correction
103 method and some uncertainty remains, especially in hazy and cloudy conditions (Nagol et al.,
104 2009). Orbital decay and changes in NOAA satellites affect AVHRR data but processed NDVI
105 data have been found to be free of trends introduced from these effects (Kaufmann et al., 2000).
106 The GIMMS dataset is comparable with NDVI products from other sensors, including MODIS,
107 SPOT VGT, SeaWIFS and Landsat ETM+ (Brown et al., 2006).

108 *2.2. Harmonic analysis of NDVI time-series*

109 Phenological patterns were extracted from the GIMMS data using a modified
110 implementation of the HANTS algorithm (Roerink et al., 2000; de Wit and Su, 2005) which
111 describes seasonal effects in vegetation using a limited number of low frequency cosine functions
112 with different phases, frequencies and amplitudes. The algorithm uses Fourier analysis,
113 complemented with detection of outliers, which are flagged and replaced iteratively (Figure 1).
114 *FIGURE 1 about here*
115 First, the raw GIMMS data are used as input for a fast Fourier transform (FFT). The
116 frequencies representing the yearly, 6-monthly and 4-monthly signals are selected from the
117 Fourier spectrum. Based on these frequencies, the spectrum is transformed back into a filtered
118 NDVI time-series using inverse FFT (iFFT). Outliers are filtered using a fit-error tolerance
119 (FET): each original NDVI value which deviates by more than the FET-value from the harmonic
120 curve is considered as noise and is replaced by the filtered value. This procedure is repeated until
121 either no points exceed the FET or a user-defined constraint is reached; the constraints concern

122 the maximum number of iterations (i_{MAX}) or a threshold on retained data points (RDP), which is
123 closely related to the degree of over-determinedness (DOD) of the model (Roerink et al., 2000).
124 The number of RDP may be taken as a measure of the performance of the model. A disadvantage
125 of HANTS is the lack of objective rules to determine its control parameters (Roerink et al.,
126 2000). Parameterization requires experience and running several parameter combinations.
127 We used HANTS in two ways. First, long-term seasonal trends were determined for each
128 pixel using the full GIMMS dataset (HA_{full}). Secondly, each year was analyzed separately
129 (HA_{year}). Differences between the two filtered results were considered NDVI anomalies (A).
130 Figure 2 and Equation 1 illustrate how the anomalies were calculated.

131 $$A(t) = HA_{year}(t) - HA_{full}(t) \qquad \text{Eq. 1}$$

132

133 *FIGURE 2 about here*

134

135 In both cases, the algorithm was tuned to disregard values lower than zero that correspond
136 to water or null-values in the GIMMS data. The eliminated values are replaced by *fills* – which
137 have a value of zero. The FET was set to 10% of the NDVI range (0.1). The number of iterations
138 required depends on the biome and the length of the time-series. For a single-year analysis, 1 or 2
139 iterations are enough for all except some tropical areas in which the amplitude is limited and
140 cloudiness affects even the fortnightly MVC images (Julien and Sobrino, 2010); in these cases a
141 stable fit is obtained after 3 or 4 iterations. The i_{MAX} was fixed to 6 iterations in the yearly
142 analysis. The full time-series is 26 times longer and it may need more iteration for a stable fit.
143 For this reason the i_{MAX} was doubled to 12. The minimal RDP was set to 16 and 416 data-points
144 for the yearly and the full datasets, respectively. This means that the output curve is always fitted

145 to at least two-thirds of the original data-points, even if the FET is not achieved. Table 1 lists the
146 parameters used for analysis of both the full dataset and each year separately.
147
148 *TABLE 1 about here*
149
150 ### *2.3. Extraction of phenological measures*
151 Various approaches have been described to derive start of growing season (SoS) from
152 NDVI time-series: half-maximum (White et al., 1997), 10% amplitude (Jönsson and Eklundh,
153 2002), inflection point (Moulin et al., 1997), maximum curvature (Zhang et al., 2003), delayed
154 moving average (DMA) and forward-looking moving average (Reed et al., 2003). We have used
155 the contribution of each Fourier component (FC) to the NDVI signal, converted into phase and
156 amplitude values, to extract measures of phenology. By way of explanation, Figure 3 shows an
157 example of a growing season in which several measures are indicated. Following White et al.
158 (2009), we used the first derivative of the HANTS-smoothed NDVI profile where SoS is defined
159 as the maximum of the first derivative (maximum NDVI increase) and the end of growing season
160 (EoS) is defined as the first point in time after SoS where the NDVI value drops below the value
161 at the start of the growing season. Between SoS and EoS, 10 equally spaced vegetation
162 development stages were then defined.
163
164 *FIGURE 3 about here*
165
166 The NDVI value at each development stage ($NDVI_{ds}$) was calculated using the yearly
167 harmonic fit (Eq. 2), where FC represents the Fourier Component, $NDVI_{mean}$ is the mean NDVI

(FC0), A is the amplitude, Φ is the phase shift and x is the day number represented in radians (Eq. 3).

$$NDVI_{ds} = NDVI_{mean} + \sum_{i=FC_1}^{FC_{max}} A_i \cdot \cos(i \cdot x + \Phi_i) \quad \text{Eq. 2}$$

$$x = day / 365 \cdot 2\pi \quad \text{Eq. 3}$$

For each growing season, this provided 12 $NDVI_{ds}$ values, which were used as input for the seasonal Mann-Kendall model.

2.4. Trend analysis

Outliers, seasonality and serial auto-correlation are characteristic of greenness data. The GIMMS data were analyzed for trends using three different strategies that take account of these effects – all involving harmonic smoothing to remove outliers and seasonality. Serial auto-correlation is assessed using auto-correlation functions (ACF) on a subset of pixels.

The first approach – here referred to as the linear model (LM) – uses the smoothed time-series (624 fortnightly values between 1981-2006) to analyze anomalies (A) between the long-term harmonic fit and yearly fits (Eq. 1). If the anomaly equals zero in any one year, then there is no trend or phase shift with respect to the long-term fit. Conversely, differences between the long-term and yearly fits might indicate land degradation or improvement, particularly if there is a significant negative or positive trend. Trends were quantified by the slope of the regression line derived from a simple linear model of the NDVI anomalies against time. Slopes obtained were tested for significance using analysis of variance (ANOVA) with a significance level (α) of 0.1 as threshold.

188 The second approach used the HANTS-interpolated data without removing seasonality. This
189 dataset violates the assumption of independent Y-values which is a basis for linear regression
190 but, in this case, the seasonal Mann-Kendall test can be used as a non-parametric test for
191 monotonic trends. Mann (1945) first suggested using the Mann-Kendall test for significance of
192 Kendall's τ for temporal trends. Later, it was extended for seasonal data, mainly in hydrological
193 analyses (Hirsch et al., 1982). The test may be used with missing or tied data and the validity
194 does not depend on the data being normally distributed; Alcaraz-Segura et al. (2009), Chamaille-
195 Jammes et al. (2006) and Pouliot et al. (2009) have previously used this approach with NDVI
196 data.

197 Given p seasons and n samples, p equals the number of observations in a year (24) and n the
198 number of years in the record (26) – which equals the number of observations for each season
199 (p). The test consists of computing the Kendall Score (S) and its variance separately for each
200 season. S is equal to the sign (sgn) of the change between subsequent samples, either -1, 0 or +1
201 (Hirsch and Slack, 1984). These individual values are summed over all samples to obtain the
202 seasonal statistic S_g (Eq. 4). The sum over all seasons provides the final test statistic S' (Eq. 5).
203 Subsequently, the Kendall's rank correlation coefficient (τ) ranging from -1 to 1 (Kendall, 1938),
204 is calculated (Eq. 6). The null hypothesis H_0 is that for each of p seasons the n samples are
205 randomly ordered (with mean $S = 0$), versus the alternative hypothesis H_A of a monotonic trend
206 in one or more seasons (Hirsch and Slack, 1984). H_0 is tested 2-sided against H_A and rejected
207 when Kendall's τ of NDVI versus time is significantly different from zero ($\alpha = 0.1$). We then
208 conclude that there *is* a monotonic trend in NDVI over time: a *greening trend* if $\tau > 0$ and a
209 *browning trend* if $\tau < 0$.

210 $$S_g = \sum_{i<j} \mathrm{sgn}(X_{jg} - X_{ig}) \qquad g = 1,2,\ldots,p \qquad \text{Eq. 4}$$

211 $$S' = \sum_{i=1}^{p} S_g$$ Eq. 5

212 $$\tau = \frac{S'}{n(n-1)/2}$$ Eq. 6

213 In a next step, the slope of this trend may be quantified using a Kendall slope estimator, but
214 we prefer the Kendall's rank correlation coefficient τ (Eq. 6).

215 The seasonal approach is a comparison of events linked to the same seasonal phase (e.g. the
216 first half of January); each scene is compared to the corresponding scene in other years but no
217 cross-phase comparisons are made. In reality, phenological cycles vary in start and length due to
218 weather variability (Cleland et al., 2007; Moulin et al., 1997; Zhou et al., 2001). This may be
219 confused with land degradation, so we propose a third method in which we use the SMK method
220 to analyze trends by vegetation development stages (VDS) rather than by month or calendar day,
221 to eliminate phenological shifts and variations in LoS. A linear model of yearly LoS values was
222 used to find regions where greening or browning may be caused by a longer or shorter thermal
223 growing season, and the coefficient of variation (CoV) was used as a measure of reliability. A
224 large variation in the identified LoS might indicate limitations to the model's capability to extract
225 phenological parameters, where reasons might be multiple growing seasons or low seasonal
226 amplitude.

227 The International Geosphere-Biosphere Program (IGBP) global land cover characteristics
228 database (Loveland et al., 2000) was used to calculate statistics per biome. The 1km dataset was
229 re-sampled to 8km resolution; the IGBP biome (Table 2) with the highest occurrence was then
230 assigned to each pixel. To minimize edge-effects and mixed pixels, only regions larger than 50
231 adjacent pixels were used to calculate statistics.

232

233 *TABLE 2 about here*

234

235 ## 3. Results

236 ### *3.1. Linear trends in NDVI anomalies*

237 Figure 4a shows the average auto-correlation function (ACF) for subsets of single and
238 double growing seasons; it confirms two types of serial autocorrelation within the data. The
239 seasonal signal is visible for time-lags of 6 months or 1 year. For short time-lags the ACF shows
240 that NDVI values are partly dependent on neighbouring values. Seasonality is considerably
241 reduced in the anomaly data (Figure 4b) but serial auto-correlation for short time-lags remains
242 unaffected by this procedure, suggesting that the power of the linear model may be
243 overestimated.

244

245 *FIGURE 4 about here*

246

247 Figure 5a shows the results of the per-pixel linear trend analysis based on the anomaly
248 dataset: green and red colours show greening and browning, respectively; areas with little or no
249 vegetation (NDVI < 0.1) are masked. The general picture is one of greening, especially in the
250 Northern Hemisphere – notably in the boreal forests, eastern Europe, Asia Minor, the Sahel, and
251 western India. In the southern hemisphere, greening is apparent in Western Australia and

252 Botswana; and browning in the tropical Africa and Indonesia / Oceania and in northern
253 Argentina.

254

255 *FIGURE 5 about here*

256

257 *3.2. Seasonal trends in interpolated NDVI*

258 The result of the SMK model (Figure 5b) shows some of the same prominent regions of
259 greening as the linear model, including western India and the Sahel, but it shows a different
260 picture for some other regions; in some cases the trend is even inverted (e.g. parts of Botswana,
261 Nigeria, Argentina and Australia). With a few exceptions, the absolute Kendall τ scores are not
262 higher than 0.25, which indicates rather weak trends.

263 The extent to which the SMK model is influenced by phenological variations is determined
264 by the variation in SoS (phenological shift) and LoS (variation in length). If the growing season
265 is stable, then the inter-annual VDS dates are close to each other – which is essential for the
266 SMK model. Figure 6 shows the variation in LoS using the slope of the linear trend (days/year)
267 analysis and the CoV. It is clear that the growing season is not stable everywhere: most regions
268 show a positive or negative trend in LoS. There are few regions where this trend is significant at
269 a p-value of α=0.1. These regions include parts of the Sahel, Asia, North-America and northern
270 Europe, with lowest p-values in Sweden and Russia. The CoV values indicate that the extraction
271 of LoS is stable (low CoV) in most parts of the northern hemisphere, but less around the tropics
272 and some parts of the southern hemisphere.

273

FIGURE 6 about here

3.3. Seasonal trends in phenology-adjusted NDVI

The map of Kendall's τ scores from the VDS model (Figure 5c) also identifies the areas of prominent greening but the absolute Kendall τ values are higher than those from the SMK model (commonly higher than 0.3 in areas with a greening or browning trend, which suggests that the trends are more significant). Results from the VDS model should be interpreted in combination with the trend in LoS (Figure 6) because greening might be caused by either a longer growing season or higher rate of production. The former effect is not captured by this method because the data have been adjusted for changes in length of growing season.

3.4. Significance of trends

In Figure 7, green and brown colours show significant trends ($\alpha = 0.1$), green indicates a positive trend and brown a negative trend. The ANOVA of the LM results show that the identified trends are significant in large parts of Europe, western India, Western Australia, the Sahel and Botswana and in some parts of Argentina, North America and Canada. Trends tend not to be significant in most tropical and tundra regions. The SMK model shows not-significant values in most parts of the world and, therefore, is not shown in Figure 7; significant values occur in western India, Western Australia and parts of the Sahel and Asia Minor. The VDS model is more powerful in rejecting the no-trend hypothesis: significant trends are detected in the northern parts of the Sahel, Asia Minor, Scandinavia, Western Australia and Botswana and smaller parts of western India, China, Canada and the Horn of Africa (Figure 7b).

FIGURE 7 about here

297

298 ## 4. Discussion

299 ### *4.1. Model results*

300 In general, the LM slopes detected by our procedure using fortnightly NDVI values are very
301 close to the linear trend analysis of yearly cumulative values published by Bai et al. (2008). On
302 average, the absolute difference in trend is < 0.001 units/year and never as much as 0.01
303 units/year – which supports the contention that reducing the temporal resolution to yearly values
304 and the choice of annual break-point does not affect the trend slopes (Dent et al., 2009), given
305 that the time-series start and end in the same phase.

306 The SMK model is valid only when it is conceptually correct to compare measurements
307 based on calendar date. In case of NDVI time-series, this assumes that no phenological shift or
308 variation in length of growing season occurs throughout the measured period – which is not the
309 case as we see from the LoS analysis. This has affected the SMK result, which identified only the
310 most conspicuous greening regions. The likeliness (according to Kendall's τ) and significance
311 (according to p-values) are generally low.

312 In the VDS model, Kendall's τ values were higher and p-values lower than in the SMK
313 approach, but it measures a different attribute of vegetation. The LM and SMK models use values
314 with equal intervals (continuous fortnightly measurements), whereas the VDS model is based on
315 an equal number of values for each growing season (the interval between these values might
316 differ between years). Therefore, the VDS model does not show greening or browning due to a
317 variation in thermal growing season; this analysis is a measure of productivity within a growing
318 season (changes in photosynthetic intensity) rather than of the total yearly productivity (changes

319 in integrated NDVI). To obtain an indication of productivity, results from the VDS model should
320 be interpreted together with variability in LoS.

321 *4.2. Biome stratification*

322 When the model results are summarized by IGBP biomes, the LM indicates overall
323 greening in all biomes except deciduous needle-leaved forest, where no trend is observed (Figure
324 9a). Figures 9b,e show that the LoS trend opposes the photosynthetic intensity trend in all
325 biomes, except shrublands and savannas. For croplands, the LoS trend is negligible. The VDS
326 model indicates a decrease in photosynthetic intensity in all forest types, which is
327 counterbalanced by an overall increase in LoS. This might indicate that vegetation growth is no
328 longer limited by temperature, but by other limiting factors such as exhaustion of soil water or
329 nutrients, which is in line with evapo-transpiration models (Zhang et al., 2009); the strongest
330 indication of this phenomenon is in the Scandinavian boreal forest (Figures 5 and 7b). On the
331 other hand, the significance of the trends is the highest outside of the forest biomes (Figure 9d)
332 but, as already remarked, the power of the LM might be over-estimated. The predictive power of
333 the models used and the performance of HANTS are discussed in Section 4.4.

334

335 *FIGURE 9 about here*

336

337 *4.3. Comparison with regional studies*

338 All three methods agree on a significant greening trend across western India, Western
339 Australia, Asia Minor and parts of the Sahel but, even here, field validation of changes of
340 vegetation over a 30-years period at 8km spatial resolution is not feasible. Even if field

observations are available, they are usually limited to points in time and may not be representative for 8km pixels (Running and Nemani, 1988). We can only compare our results with other regional studies.

A problem inherent to the use of time-series of data is that the initial status, in this case of land degradation, is often not known. In the 1970s and, again, in the early 1980s, the Sahel experienced severe droughts (Govaerts and Lattanzio, 2008; Nicholson, 2000) from which the recovery shows as a greening trend. Greening of the Sahel is confirmed by several studies (Anyamba and Tucker, 2005; Herrmann et al., 2005; Heumann et al., 2007; Olsson et al., 2005) but there is debate about the role of human-induced land degradation (Hein and de Ridder, 2006; Prince et al., 2007). Greening in the thorn forests of the west-Indian Deccan can be explained, in part, by recovery from overgrazing that occurred prior to the start of the GIMMS record; large parts of these shrublands are now protected.

Donohue et al. (2009) identified greening in Western Australia by an increase in fPAR (from AVHRR PAL) for the period 1981-2006; greening in north-eastern Australia is also in line with the increase in fPAR. In contrast, browning has taken place in central Australia; according to Nemani et al. (2003), this might be explained by an 0.1 ºC/y increase in temperature. Also in the southern hemisphere, there has been greening in Botswana (although less prominent and only statistically significant in the LM and VDS models), which is in line with the 1% yearly increase in NPP found by Nemani et al. (2003), using AVHRR data in a production-efficiency model.

In Canada, all models show three regions of greening: (1) the North-western and Yukon tundra, (2) east of Hudson Bay, and (3) southern Saskatchewan. These trends are most explicit in the VDS model and confirmed by other studies. Pouliot et al. (2009) used a similar Mann-Kendall approach with GIMMS data and found NDVI trends of about 0.01 units/year in all three

regions. Goetz et al. (2005), using the same input data, confirm two out of three greening regions and also browning in Alaska, close to the British Columbia / Alberta border, and some regions in Quebec. They conclude that growth in tundra has increased due to rising CO_2 concentration and temperature but, in the boreal forest, various other factors including fire are influential. This is seconded by Alcaraz-Segura et al. (2009), who also show that the GIMMS dataset largely misses greening due to post-fire recovery.

There are also regions where the three models do not agree or, even, show opposite trends. One is southern Chile, where the LM shows significant greening. Although there seems to be a small increase in NPP due to an increase in solar radiation (Nemani et al., 2003), the linear model is not supported by the other two or by a study of changes in NDVI over South America by Paruelo et al. (2004) – who did find a positive slope in APAR between 1981 and 2000, but not as far south as the linear model. Contrarily, the SMK model shows a browning trend. The VDS model does not show the extensive greening indicated by the linear model or the browning indicated by the SMK model. The greening in central Argentina, west of Buenos Aires (Paruelo et al., 2004), which is in line with an identified increase in humidity (Nemani et al., 2003), is only identified by the VDS model.

There is also some discrepancy in trends in Eurasia. According to the LM, greening prevails over browning, most conspicuously towards the east. This is in line with the relation between PAL NDVI and Land Surface Temperature (Julien et al., 2006) – drier areas in the south have become hotter and even drier while northern Europe has become cooler. Stöckli and Vidale (2004) found a related positive trend in LoS of 1.4 days per year in central Europe (Germany) and a negative trend of -0.54 days per year in Scandinavia but our harmonic analysis shows an increase in LoS in Scandinavia (Figure 6), which might indicate warming (Hüttich et al., 2007; Karlsen et al., 2007). A longer growing season would explain the differences between the LM

388 and the VDS model. Greening due to a longer growing season does not necessarily affect the
389 intensity of activity in the growing season; the VDS model shows a decline in activity in
390 Scandinavia, whereas the LM shows a slight increase.

391 In their global assessment and in detail in China, Bai and Dent (2009) and Bai et al. (2008)
392 used GIMMS data in another way to assess land degradation and improvement. They used a
393 linear model but introduced additional criteria of rain-use efficiency and energy-use efficiency to
394 screen NDVI trends caused by drought and climatic warming. By translating NDVI to net
395 primary productivity (NPP) using the relationship with MODIS NPP data, they derived a tangible
396 measure of severity that can be subjected to economic appraisal. For China, they conclude that
397 land degradation is most conspicuous in the rapidly-developing, humid south, rather than in the
398 drylands of the north and west, where major reclamation initiatives have concentrated. Both the
399 LM and the VDS model support this conclusion. A study using GIMMS and SPOT VGT in the
400 Chinese Loess Plateau found a similar relationship between rainfall and land degradation (Xin et
401 al., 2008). The spatial pattern of correlation between NDVI and time (1981-2003) is best
402 reproduced by using the VDS model (Figure 8).

403

404 *FIGURE 8 about here*

405

406 *4.4. Limitations and lessons learned*

407 Harmonic analysis has solved or, at least, mitigated some limitations of previous work that
408 used only yearly-accumulated NDVI data. The HANTS procedure removes cloud interference
409 and eliminates the influence of phenological shift between the northern and southern

410 hemispheres, but does not affect inter-annual phenological shifts from which the LM and,
411 especially, the SMK model suffer. This problem is solved by the single-growing-season
412 normalization used in the VDS dataset.

413 Serial autocorrelation remains an issue with the use of the linear model (Figure 4); a
414 deviation from the long-term is likely to show for an entire growing season, or at least a part of
415 it, rather than for a single measurement. Providing that seasonality is accounted for, the power of
416 the statistical methods is mainly determined by the sample size; serial auto-correlation will be an
417 issue if the value of a sample is partly determined by its neighbouring samples. A dataset with
418 serial auto-correlation contains less information than one of the same length with truly
419 independent samples so serial auto-correlation falsely inflates the power of the test (McBride et
420 al., 1994). Therefore, it is a challenge to distinguish between *statistically significant changes* and
421 *practically significant changes*. In this sense, non-parametric models should be more robust than
422 parametric models or, from a different perspective, the linear trend is more powerful in rejecting
423 H_0 (Hirsch and Slack, 1984), which explains why the LM trends appear more significant (Figure
424 7, Figure 9d).

425 The performance of HANTS is biome dependent. Most IGBP biomes show harmonic fits
426 with more than 90% retained data points (Figure 9c) so the NDVI curve is reproduced, losing less
427 than 10% of the original measurements. Exceptions are evergreen broadleaf forest (tropics),
428 deciduous needle-leaf forest and shrublands, which – in the IGBP classification (Table 2) –
429 includes most tundra ecosystems where NDVI is zero (or a *fill value* in the GIMMS data) under
430 snow cover and increases quickly to high values upon snowmelt. The tundra situation would be
431 better described by double logistic fitting (Beck et al., 2006). In contrast, NDVI is high
432 throughout the year in the tropics, resulting in noise in the phase-shift estimates that causes
433 inaccuracies in the extraction of phenological measures.

434 An improved analysis requires a globally applicable method for deriving the start and
435 length of growing season. With current techniques, phenological measures can be derived
436 automatically only for areas with a single annual growing season. It is hard to extract multi-
437 season measures (which are needed, for instance, in south China, the horn of Africa and the
438 Ganges-plain in India). Figure 6b shows a large coefficient of variance in the extracted LoS for
439 these regions, which might be caused by slight variations in the minimal NDVI between the
440 growing seasons. This means that, in one year, only the first season may be extracted and, in
441 another year, both seasons. It is clear that that smoothing and extraction of phenological
442 measures are neither simple nor straightforward (Hird and McDermid, 2009). Ideally, we would
443 wish to use one generally method but, although there are several methods available, each is
444 suitable for only one or few biomes; the method proposed by (Geerken, 2009), defining a set of
445 reference curves, is a step towards global application.

446 Assessment and even definition of land degradation remains contentious (de Jong et al.,
447 2010). Since the initial status is often not known, greening might represent recovery from
448 drought or other disturbance; and greening resulting from the replacement of old-growth forest
449 by crops or grassland might be considered degradation rather than land improvement (Bai et al.
450 2008). In the humid tropics, the NDVI proxy is not reliable due to saturation of the signal
451 (Myneni et al., 2002) or cloud cover. Although most trends are in line with decreasing NPP
452 (Nemani et al., 2003), there are also contradicting trends.

453 At present, choice of NDVI time-series presents a trade-off between temporal coverage and
454 spatial resolution – between 10 years at 250-500m resolution (MODIS) or almost 30 years at 1-
455 8km resolution (AVHRR). The longer period captures some climatic cycles and significant
456 changes in land use and management, but a single pixel might contain several land use types or

ecosystems. Field validation is, and will remain, unfeasible and validation by other studies is also questionable since many studies use the same NDVI data.

We have assessed monotonic trends in NDVI but vegetation trends are often complex and breaks or interruptions of trends are common (Angert et al., 2005; Slayback et al., 2003; Tucker et al., 2001; Verbesselt et al., 2010; Xin et al., 2008). Sudden trend shifts may be caused by major volcanic eruptions, large fluctuations driven by fast-acting climatic features like El Niño or broad-scale land management practices. Gradual changes may be associated with slow-acting climatic cycles or the accumulation of changes in management. These gradual changes might ultimately trigger a catastrophic shift in the ecosystem (Scheffer et al., 2001). Trend breaks will become easier to identify as the available time-series of global observations become longer.

5. Conclusions

We have used harmonic analysis to enhance linear and monotonic trend analysis of GIMMS NDVI time-series data. Greening and browning trends were revealed but cannot be quantified easily. Variations in phenology conceal simple greening or browning trends but this aspect may be illuminated by using the seasonal Mann-Kendall (SMK) model with normalization of the growing season using vegetation development stages (VDS), rather than analysis by calendar day. The likeliness of greening or browning from the VDS model showed the closest relationship to regional studies and indicates that vegetation intensity, as much as the yearly sum NDVI, may serve to indicate greening or browning. However, trends that are solely caused by variation in length of growing season are not directly detected because of the normalization procedure.

At the global scale, comparison of NDVI values by calendar date is inadequate – due to phenological shifts and variation in length of growing season – but it is difficult to extract phenological measures using a generalized method. In a next step, the explaining power of the

480 VDS model may be increased by using a more sophisticated approach to derive these measures,
481 for instance by using several extraction methods, according to the phenology or climate zone.

482 Linear model trends derived from anomalies between long-term and yearly harmonic fits
483 were hardly different from the trends of yearly averaged NDVI data. It is therefore considered
484 unlikely that averaging to cumulative values influences the trend analysis. However, the
485 explaining power will decrease with a decreasing number of observations. All models agreed on a
486 greening trend in western India, the Sahel and parts of Asia Minor, Canada, northern China and
487 Western Australia; the biomes showing most-prominent greening were shrubland, savanna and
488 cropland.

489 Acknowledgements

490 This work is partly financed through FAO contract PR35852. The authors thank Zhanguo
491 Bai for providing data and results from previous studies. We appreciate the NASA GIMMS group
492 providing the latest version of their NDVI data set.

493 References

494 Alcaraz-Segura, D., Chuvieco, E., Epstein, H.E., Kasischke, E.S., & Trishchenko, A. (2009). Debating the greening vs.
495 browning of the North American boreal forest: differences between satellite datasets. *Global Change Biology, 16*,
496 760-770.
497 Angert, A., Biraud, S., Bonfils, C., Henning, C.C., Buermann, W., Pinzon, J., Tucker, C.J., & Fung, I. (2005). Drier
498 summers cancel out the CO2 uptake enhancement induced by warmer springs. *Proceedings of the National Academy*
499 *of Sciences of the United States of America, 102*, 10823-10827.
500 Anyamba, A., & Tucker, C.J. (2005). Analysis of Sahelian vegetation dynamics using NOAA-AVHRR NDVI data from
501 1981-2003. *Journal of Arid Environments, 63*, 596-614.
502 Bai, Z., & Dent, D. (2009). Recent Land Degradation and Improvement in China. *AMBIO: A Journal of the Human*
503 *Environment, 38*, 150-156.
504 Bai, Z.G., Dent, D.L., Olsson, L., & Schaepman, M.E. (2008). Proxy global assessment of land degradation. *Soil Use and*
505 *Management, 24*, 223-234.
506 Baldocchi, D., Falge, E., Gu, L., Olson, R., Hollinger, D., Running, S., Anthoni, P., Bernhofer, C., Davis, K., & Evans, R.
507 (2001). FLUXNET: A new tool to study the temporal and spatial variability of ecosystem–scale carbon dioxide,
508 water vapor, and energy flux densities. *Bulletin of the American Meteorological Society, 82*, 2415-2434.
509 Barber, V.A., Juday, G.P., & Finney, B.P. (2000). Reduced growth of Alaskan white spruce in the twentieth century from
510 temperature-induced drought stress. *Nature, 405*, 668-673.
511 Barford, C.C., Wofsy, S.C., Goulden, M.L., Munger, J.W., Pyle, E.H., Urbanski, S.P., Hutyra, L., Saleska, S.R., Fitzjarrald,
512 D., & Moore, K. (2001). Factors Controlling Long- and Short-Term Sequestration of Atmospheric CO2 in a Mid-
513 latitude Forest. *Science, 294*, 1688-1691.

514 Beck, P.S.A., Atzberger, C., Høgda, K.A., Johansen, B., & Skidmore, A.K. (2006). Improved monitoring of vegetation
515 dynamics at very high latitudes: A new method using MODIS NDVI. *Remote Sensing of Environment, 100*, 321-334.
516 de Beurs, K.M., & Henebry, G.M. (2004). Trend analysis of the Pathfinder AVHRR Land (PAL) NDVI data for the deserts
517 of central Asia. *Geoscience and Remote Sensing Letters, IEEE, 1*, 282-286.
518 Brown, M.E., Pinzon, J.E., Didan, K., Morisette, J.T., & Tucker, C.J. (2006). Evaluation of the consistency of long-term
519 NDVI time series derived from AVHRR,SPOT-vegetation, SeaWiFS, MODIS, and Landsat ETM+ sensors. *IEEE*
520 *Transactions on Geoscience and Remote Sensing, 44*, 1787-1793.
521 Cai, X.L., & Sharma, B.R. (2010). Integrating remote sensing, census and weather data for an assessment of rice yield,
522 water consumption and water productivity in the Indo-Gangetic river basin. *Agricultural Water Management, 97*,
523 309-316.
524 Chamaille-Jammes, S., Fritz, H., & Murindagomo, F. (2006). Spatial patterns of the NDVI-rainfall relationship at the
525 seasonal and interannual time scales in an African savanna. *International Journal of Remote Sensing, 27*, 5185-5200.
526 Cleland, E.E., Chuine, I., Menzel, A., Mooney, H.A., & Schwartz, M.D. (2007). Shifting plant phenology in response to
527 global change. *Trends in Ecology & Evolution, 22*, 357-365.
528 Cracknell, A.P. (2001). The exciting and totally unanticipated success of the AVHRR in applications for which it was never
529 intended. *Advances in Space Research, 28*, 233-240.
530 Dent, D.L., Bai, Z.G., Schaepman, M.E., & Olsson, L. (2009). Letter to the Editor, Response to Wessels: Comments on
531 'Proxy global assessment of land degradation'. *Soil Use and Management, 25*, 93-97.
532 Doktor, D., Bondeau, A., Koslowski, D., & Badeck, F.-W. (2009). Influence of heterogeneous landscapes on computed
533 green-up dates based on daily AVHRR NDVI observations. *Remote Sensing of Environment, 113*, 2618-2632.
534 Donohue, R.J., McVicar, T.R., & Roderick, M.L. (2009). Climate-related trends in Australian vegetation cover as inferred
535 from satellite observations, 1981–2006. *Global Change Biology, 15*, 1025-1039.
536 Foley, J.A., Levis, S., Costa, M.H., Cramer, W., & Pollard, D. (2000). Incorporating dynamic vegetation cover within
537 global climate models. *Ecological Applications, 10*, 1620-1632.
538 Geerken, R.A. (2009). An algorithm to classify and monitor seasonal variations in vegetation phenologies and their inter-
539 annual change. *ISPRS Journal of Photogrammetry and Remote Sensing, 64*, 422-431.
540 Goetz, S.J., Bunn, A.G., Fiske, G.J., & Houghton, R.A. (2005). Satellite-observed photosynthetic trends across boreal North
541 America associated with climate and fire disturbance. *Proceedings of the National Academy of Sciences of the*
542 *United States of America, 102*, 13521-13525.
543 Goulden, M.L., Munger, J.W., Fan, S.-M., Daube, B.C., & Wofsy, S.C. (1996). Exchange of Carbon Dioxide by a
544 Deciduous Forest: Response to Interannual Climate Variability. *Science, 271*, 1576-1578.
545 Govaerts, Y., & Lattanzio, A. (2008). Estimation of surface albedo increase during the eighties Sahel drought from
546 Meteosat observations. *Global and Planetary Change, 64*, 139-145.
547 Hein, L., & de Ridder, N. (2006). Desertification in the Sahel: a reinterpretation. *Global Change Biology, 12*, 751 - 758.
548 Herrmann, S.M., Anyamba, A., & Tucker, C.J. (2005). Recent trends in vegetation dynamics in the African Sahel and their
549 relationship to climate. *Global Environmental Change Part A, 15*, 394-404.
550 Heumann, B.W., Seaquist, J.W., Eklundh, L., & Jönsson, P. (2007). AVHRR derived phenological change in the Sahel and
551 Soudan, Africa, 1982–2005. *Remote Sensing of Environment, 108*, 385 - 392.
552 Hird, J.N., & McDermid, G.J. (2009). Noise reduction of NDVI time series: An empirical comparison of selected
553 techniques. *Remote Sensing of Environment, 113*, 248-258.
554 Hirsch, R.M., & Slack, J.R. (1984). A nonparametric trend test for seasonal data with serial dependence. *Water Resources*
555 *Research, 20*, 727-732.
556 Hirsch, R.M., Slack, J.R., & Smith, R.A. (1982). Techniques of trend analysis for monthly water quality data. *Water*
557 *Resources Research, 18*, 107-121.
558 Holben, B.N. (1986). Characteristics of maximum-value composite images from temporal AVHRR data. *International*
559 *Journal of Remote Sensing, 7*, 1417-1434.
560 Hussian, M., Grimvall, A., Burdakov, O., & Sysoev, O. (2005). Monotonic regression for the detection of temporal trends in
561 environmental quality data. *Match, 54*, 535-550.
562 Hüttich, C., Herold, M., Schmullius, C., Egorov, V., & Bartalev, S.A. (2007). Indicators of Northern Eurasia's land-cover
563 change trends from SPOT-VEGETATION time-series analysis 1998-2005. *International Journal of Remote Sensing,*
564 *28*, 4199-4206.
565 IPCC (2007). Synthesis Report. In, *4th Assessment Report of the Intergovernmental Panel on Climate Change* (p. 52)
566 de Jong, R., de Bruin, S., Schaepman, M.E., & Dent, D.L. (2010). Quantitative mapping of global land degradation using
567 Earth observations. *International Journal of Remote Sensing, submitted*
568 Jönsson, P., & Eklundh, L. (2002). Seasonality extraction by function fitting to time-series of satellite sensor data.
569 *Geoscience and Remote Sensing, IEEE Transactions on, 40*, 1824-1832.
570 Julien, Y., & Sobrino, J.A. (2010). Comparison of cloud-reconstruction methods for time series of composite NDVI data.
571 *Remote Sensing of Environment, 114*, 618-625.

572 Julien, Y., Sobrino, J.A., & Verhoef, W. (2006). Changes in land surface temperatures and NDVI values over Europe
573 between 1982 and 1999. *Remote Sensing of Environment, 103*, 43-55.
574 Justice, C.O., Townshend, J.R.G., Holben, B.N., & Tucker, C.J. (1985). Analysis of the phenology of global vegetation
575 using meteorological satellite data. *International Journal of Remote Sensing, 6*, 1271-1318.
576 Karlsen, S.R., Solheim, I., Beck, P.S.A., Høgda, K.A., Wielgolaski, F.E., & Tommervik, H. (2007). Variability of the start
577 of the growing season in Fennoscandia, 1982–2002. *International Journal of Biometeorology, 51*, 513-524.
578 Kaufmann, R.K., Zhou, L., Knyazikhin, Y., Shabanov, V., Myneni, R.B., & Tucker, C.J. (2000). Effect of orbital drift and
579 sensor changes on the time series of AVHRR vegetation index data. *IEEE Transactions on Geoscience and Remote*
580 *Sensing, 38*, 2584-2597.
581 Kendall, M.G. (1938). A New Measure of Rank Correlation. *Biometrika, 30*, 81-93.
582 Liang, L., & Schwartz, M. (2009). Landscape phenology: an integrative approach to seasonal vegetation dynamics.
583 *Landscape Ecology, 24*, 465-472.
584 Loveland, T.R., Reed, B.C., Brown, J.F., Ohlen, D.O., Zhu, Z., Yang, L., & Merchant, J.W. (2000). Development of a
585 global land cover characteristics database and IGBP DISCover from 1 km AVHRR data. *International Journal of*
586 *Remote Sensing, 21*, 1303-1330.
587 Mann, H.B. (1945). Nonparametric Tests Against Trend. *Econometrica, 13*, 245-259.
588 McBride, G.B., Loftis, J.C., & Hamilton, N.Z. (1994). The most important statistical aspects. In Adriaanse (Ed.),
589 *Proceedings of the International Workshop Monitoring Tailor-Made* (pp. 153-161). Beekbergen, The Netherlands
590 Menzel, A., Sparks, T.H., Estrella, N., Koch, E., Aasa, A., Ahas, R., Alm-Kubler, K., Bissolli, P., Braslavska, O., Briede,
591 A., Chmielewski, F.M., Crepinsek, Z., Curnel, Y., Dahl, A., Defila, C., Donnelly, A., Filella, Y., Jatczak, K., Mage,
592 F., Mestre, A., Nordli, Ø., Penuelas, J., Pirinen, P., Remisova, V., Scheifinger, H., Striz, M., Susnik, A., van Vliet,
593 A.J.H., Wielgolaski, F.-E., Zach, S., & Zust, A. (2006). European phenological response to climate change matches
594 the warming pattern. *Global Change Biology, 12*, 1969-1976.
595 Metternicht, G., Zinck, J.A., Blanco, P.D., & Del Valle, H.F. (2010). Remote sensing of land degradation: Experiences from
596 Latin America and the Caribbean. *Journal of Environmental Quality, 39*, 42-61.
597 Moulin, S., Kergoat, L., Viovy, N., & Dedieu, G. (1997). Global-Scale Assessment of Vegetation Phenology Using
598 NOAA/AVHRR Satellite Measurements. *Journal of Climate, 10*, 1154-1170.
599 Myneni, R.B., Hoffman, S., Knyazikhin, Y., Privette, J.L., Glassy, J., Tian, Y., Wang, Y., Song, X., Zhang, Y., Smith, G.R.,
600 Lotsch, A., Friedl, M., Morisette, J.T., Votava, P., Nemani, R.R., & Running, S.W. (2002). Global products of
601 vegetation leaf area and fraction absorbed PAR from year one of MODIS data. *Remote Sensing of Environment, 83*,
602 214-231.
603 Myneni, R.B., Keeling, C.D., Tucker, C.J., Asrar, G., & Nemani, R.R. (1997). Increased plant growth in the northern high
604 latitudes from 1981 to 1991. *Nature, 386*, 698-702.
605 Nagol, J.R., Vermote, E.F., & Prince, S.D. (2009). Effects of atmospheric variation on AVHRR NDVI data. *Remote Sensing*
606 *of Environment, 113*, 392-397.
607 Nemani, R.R., Keeling, C.D., Hashimoto, H., Jolly, W.M., Piper, S.C., Tucker, C.J., Myneni, R.B., & Running, S.W.
608 (2003). Climate-Driven Increases in Global Terrestrial Net Primary Production from 1982 to 1999. *Science, 300*,
609 1560-1563.
610 Nicholson, S. (2000). Land surface processes and Sahel climate. *Reviews of Geophysics, 38*, 117–138.
611 Olsson, L., Eklundh, L., & Ardö, J. (2005). A recent greening of the Sahel -- trends, patterns and potential causes. *Journal*
612 *of Arid Environments, 63*, 556-566.
613 Paruelo, J.M., Garbulsky, M.F., Guerschman, J.P., & Jobbágy, E.G. (2004). Two decades of Normalized Difference
614 Vegetation Index changes in South America: identifying the imprint of global change. *International Journal of*
615 *Remote Sensing, 25*, 2793 - 2806.
616 Pouliot, D., Latifovic, R., & Olthof, I. (2009). Trends in vegetation NDVI from 1 km AVHRR data over Canada for the
617 period 1985-2006. *International Journal of Remote Sensing, 30*, 149-168.
618 Prince, S.D., Wessels, K.J., Tucker, C.J., & Nicholson, S.E. (2007). Desertification in the Sahel: a reinterpretation of a
619 reinterpretation. *Global Change Biology, 13*, 1308-1313.
620 Reed, B.C., White, M., & Brown, J.F. (2003). Remote sensing phenology. In M.D. Schwartz (Ed.), *Phenology: An*
621 *Integrative Environmental Science* (pp. 365–381). Dordrecht, The Netherlands: Kluwer Academic Publishing.
622 Roerink, G.J., Menenti, M., & Verhoef, W. (2000). Reconstructing cloudfree NDVI composites using Fourier analysis of
623 time series. *International Journal of Remote Sensing, 21*, 1911 - 1917.
624 Running, S.W., & Nemani, R.R. (1988). Relating seasonal patterns of the AVHRR vegetation index to simulated
625 photosynthesis and transpiration of forests in different climates. *Remote Sensing of Environment, 24*, 347-367.
626 Scheffer, M., Carpenter, S., Foley, J.A., Folke, C., & Walker, B. (2001). Catastrophic shifts in ecosystems. *Nature, 413*,
627 591-596.
628 Sims, D.A., Rahman, A.F., Cordova, V.D., El-Masri, B.Z., Baldocchi, D.D., Bolstad, P.V., Flanagan, L.B., Goldstein, A.H.,
629 Hollinger, D.Y., Misson, L., Monson, R.K., Oechel, W.C., Schmid, H.P., Wofsy, S.C., & Xu, L. (2008). A new

model of gross primary productivity for North American ecosystems based solely on the enhanced vegetation index and land surface temperature from MODIS. *Remote Sensing of Environment, 112*, 1633-1646.
Slayback, D.A., Pinzon, J.E., Los, S.O., & Tucker, C.J. (2003). Northern hemisphere photosynthetic trends 1982-99. *Global Change Biology, 9*, 1-15.
Stöckli, R., & Vidale, P.L. (2004). European plant phenology and climate as seen in a 20-year AVHRR land-surface parameter dataset. *International Journal of Remote Sensing, 25*, 3303 - 3330.
Tucker, C., Pinzon, J., Brown, M., Slayback, D., Pak, E., Mahoney, R., Vermote, E., & El Saleous, N. (2005). An extended AVHRR 8km NDVI dataset compatible with MODIS and SPOT vegetation NDVI data. *International Journal of Remote Sensing, 26*, 4485-4498.
Tucker, C.J. (1979). Red and photographic infrared linear combinations for monitoring vegetation. *Remote Sensing of Environment, 8*, 27-150.
Tucker, C.J., Pinzon, J.E., & Brown, M.E. (2004). Global Inventory Modeling and Mapping Studies, NA94apr15b.n11-VIg, 2.0, Global Land Cover Facility, University of Maryland, College Park, Maryland.
Tucker, C.J., Slayback, D.A., Pinzon, J.E., Los, S.O., Myneni, R.B., & Taylor, M.G. (2001). Higher northern latitude normalized difference vegetation index and growing season trends from 1982 to 1999. *International Journal of Biometeorology, 45*, 184-190.
UNEP (2007). *Global Environment Outlook (GEO) 4*. Nairobi: UNEP.
Verbesselt, J., Hyndman, R., Newnham, G., & Culvenor, D. (2010). Detecting trend and seasonal changes in satellite image time series. *Remote Sensing of Environment, 114*, 106-115.
Wessels, K.J. (2009). Letter to the Editor: comments on 'Proxy global assessment of land degradation'. *Soil Use and Management, 25*, 91-92.
Westerling, A.L., Hidalgo, H.G., Cayan, D.R., & Swetnam, T.W. (2006). Warming and Earlier Spring Increase Western U.S. Forest Wildfire Activity. *Science, 313*, 940-943.
White, M.A., de Beurs, K.M., Didan, K., Inouye, D.W., Richardson, A.D., Jensen, O.P., Magnuson, J., O'Keefe, J., Zhang, G., Nemani, R.R., van Leeuwen, W.J.D., Brown, J.F., de Wit, A., Schaepman, M.E., Lin, X., Dettinger, M., Bailey, A., Kimball, J., Schwartz, M.D., Baldocchi, D.D., Lee, J.T., & Lauenroth, W.K. (2009). Intercomparison, interpretation, and assessment of spring phenology in North America estimated from remote sensing for 1982–2006. *Global Change Biology, 15*, 2335-2359.
White, M.A., Running, S.W., & Thornton, P.E. (1999). The impact of growing-season length variability on carbon assimilation and evapotranspiration over 88 years in the eastern US deciduous forest *International Journal of Biometeorology, 42*, 139-145.
White, M.A., Thornton, P.E., & Running, S.W. (1997). A continental phenology model for monitoring vegetation responses to interannual climatic variability. *Global Biogeochemical Cycles, 11*, 217-234.
de Wit, A.J.W., & Su, B. (2005). Deriving phenological indicators from SPOT-VGT data using the HANTS algorithm. In, *2nd international SPOT-VEGETATION user conference* (pp. 195-201). Antwerp, Belgium
Xin, Z., Xu, J., & Zheng, W. (2008). Spatiotemporal variations of vegetation cover on the Chinese Loess Plateau (1981—2006): Impacts of climate changes and human activities. *Science in China Series D: Earth Sciences, 51*, 67 - 78.
Yu, D., Shi, P., Shao, H., Zhu, W., & Pan, Y. (2009). Modelling net primary productivity of terrestrial ecosystems in East Asia based on an improved CASA ecosystem model. *International Journal of Remote Sensing, 30*, 4851-4866.
Zhang, K., Kimball, J.S., Mu, Q., Jones, L.A., Goetz, S.J., & Running, S.W. (2009). Satellite based analysis of northern ET trends and associated changes in the regional water balance from 1983 to 2005. *Journal of Hydrology, 379*, 92-110.
Zhang, X., Friedl, M.A., Schaaf, C.B., Strahler, A.H., Hodges, J.C.F., Gao, F., Reed, B.C., & Huete, A. (2003). Monitoring vegetation phenology using MODIS. *Remote Sensing of Environment, 84*, 471-475.
Zhou, L., Tucker, C.J., Kaufmann, R.K., Slayback, D.A., Shabanov, N.V., & Myneni, R.B. (2001). Variations in northern vegetation activity inferred from satellite data of vegetation index during 1981 to 1999. *Journal of Geophysical Research, 106*, 20269-20283.
Zika, M., & Erb, K.H. (2009). The global loss of net primary production resulting from human-induced soil degradation in drylands. *Ecological Economics, 69*, 310-318.

List of Tables

List of Figures

TABLES

Table 1 Parameters used in HANTS analysis.

	Single-year	Full GIMMS (26 years)
Number of data points	26	624
Fourier Frequencies	0,1,2,3	0,26,52,78
Fit Error Tolerance (FET)	0.1	0.1
Max. Iterations (i_{MAX})	6	12
Min. Retained data points	16 (66,7%)	416 (66,7%)

727
728 Table 2 IGBP DISCover Land Cover Classification System (Loveland et al., 2000).
729

Code	Class name
1	Evergreen Needleleaf Forest
2	Evergreen Broadleaf Forest
3	Deciduous Needleleaf Forest
4	Deciduous Broadleaf Forest
5	Mixed Forests
6	Closed Shrublands
7	Open Shrublands
8	Woody Savannas
9	Savannas
10	Grasslands
11	Persistent Wetlands
12	Croplands
13	Urban and Built-Up
14	Cropland/Other Vegetation Mosaic
15	Snow and Ice
16	Barren or Sparsely Vegetated
17	Water

730
731

Figure1
Click here to download high resolution image

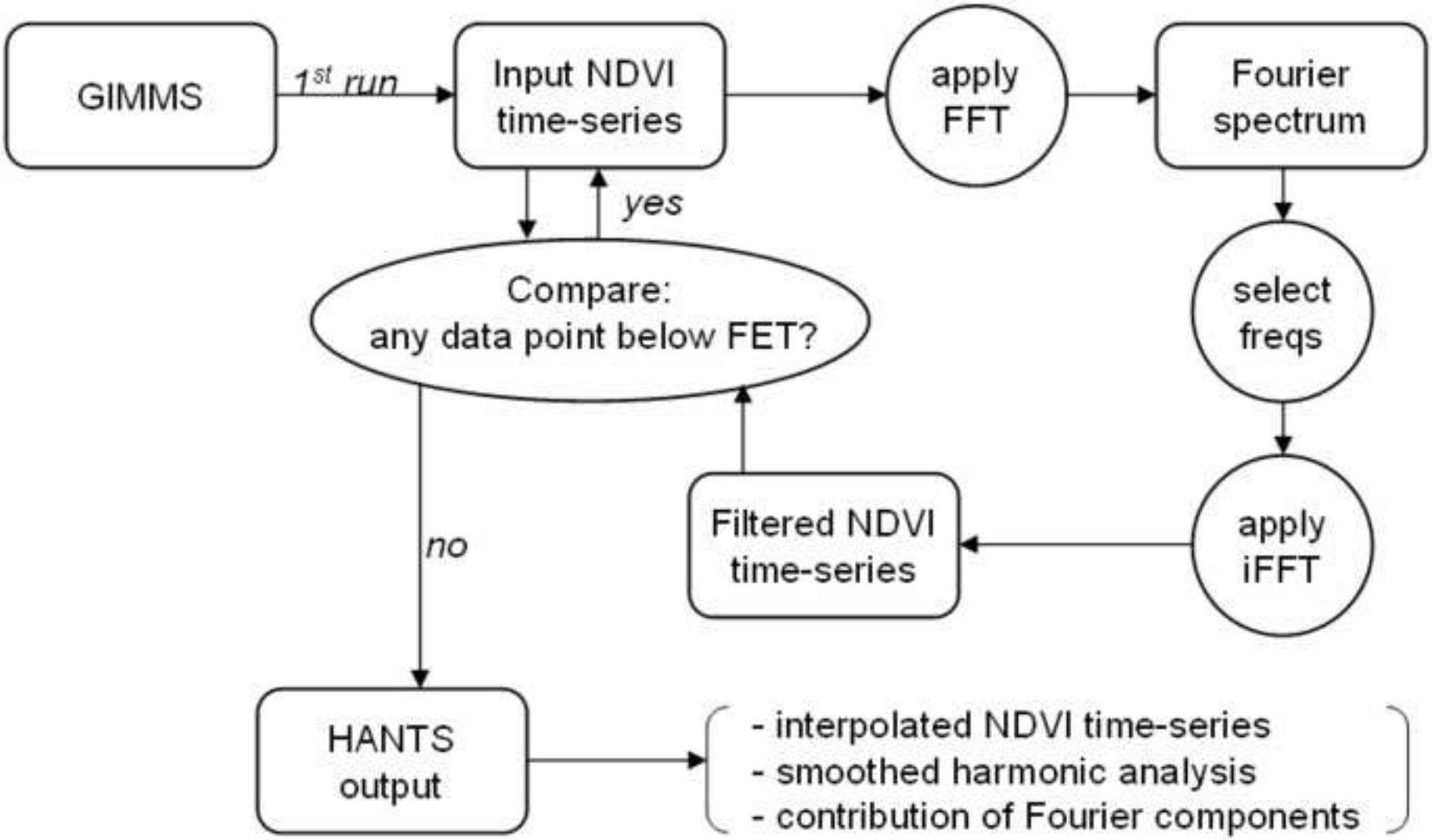

Figure2

Click here to download high resolution image

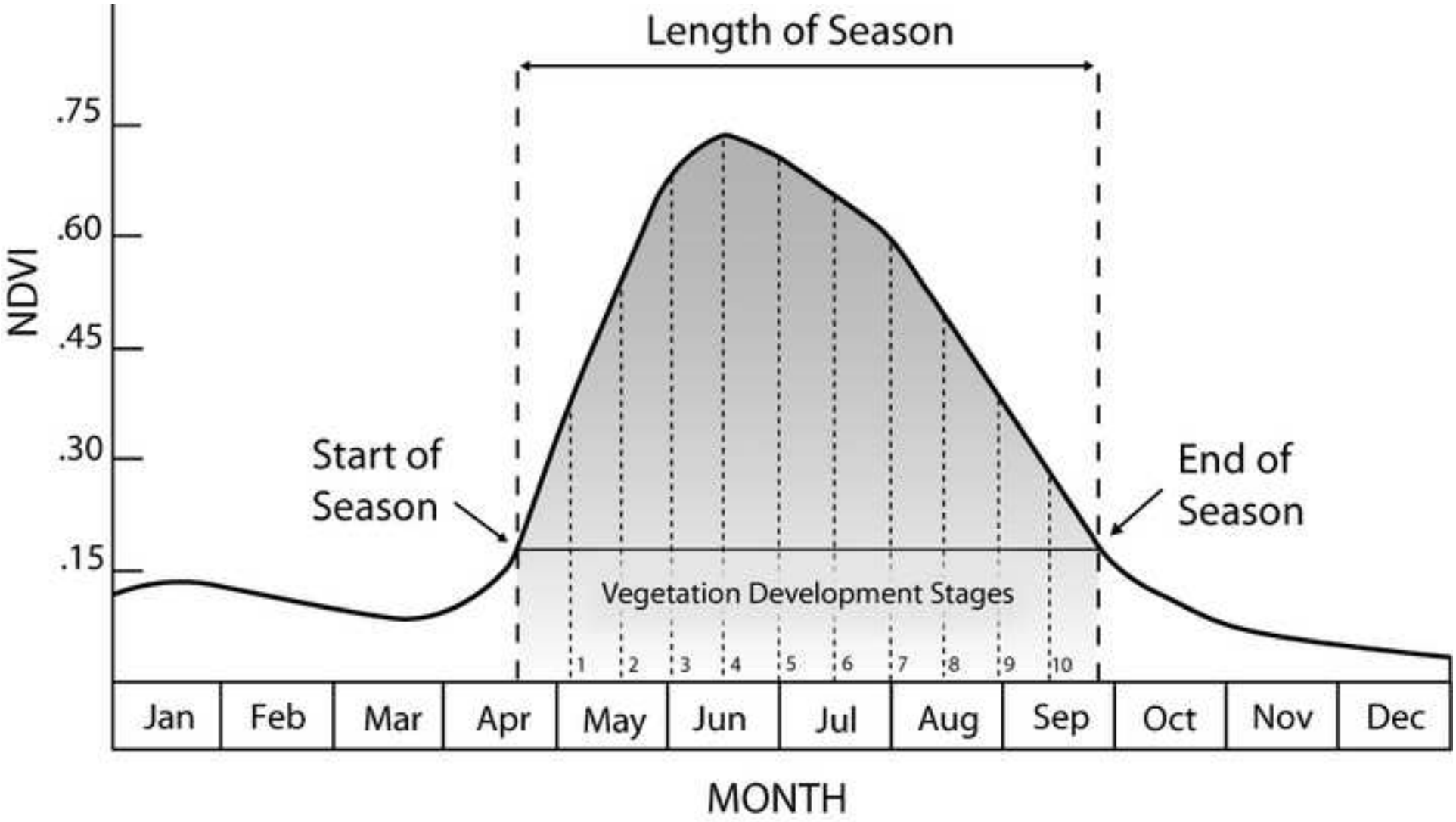

Figure3

Click here to download high resolution image

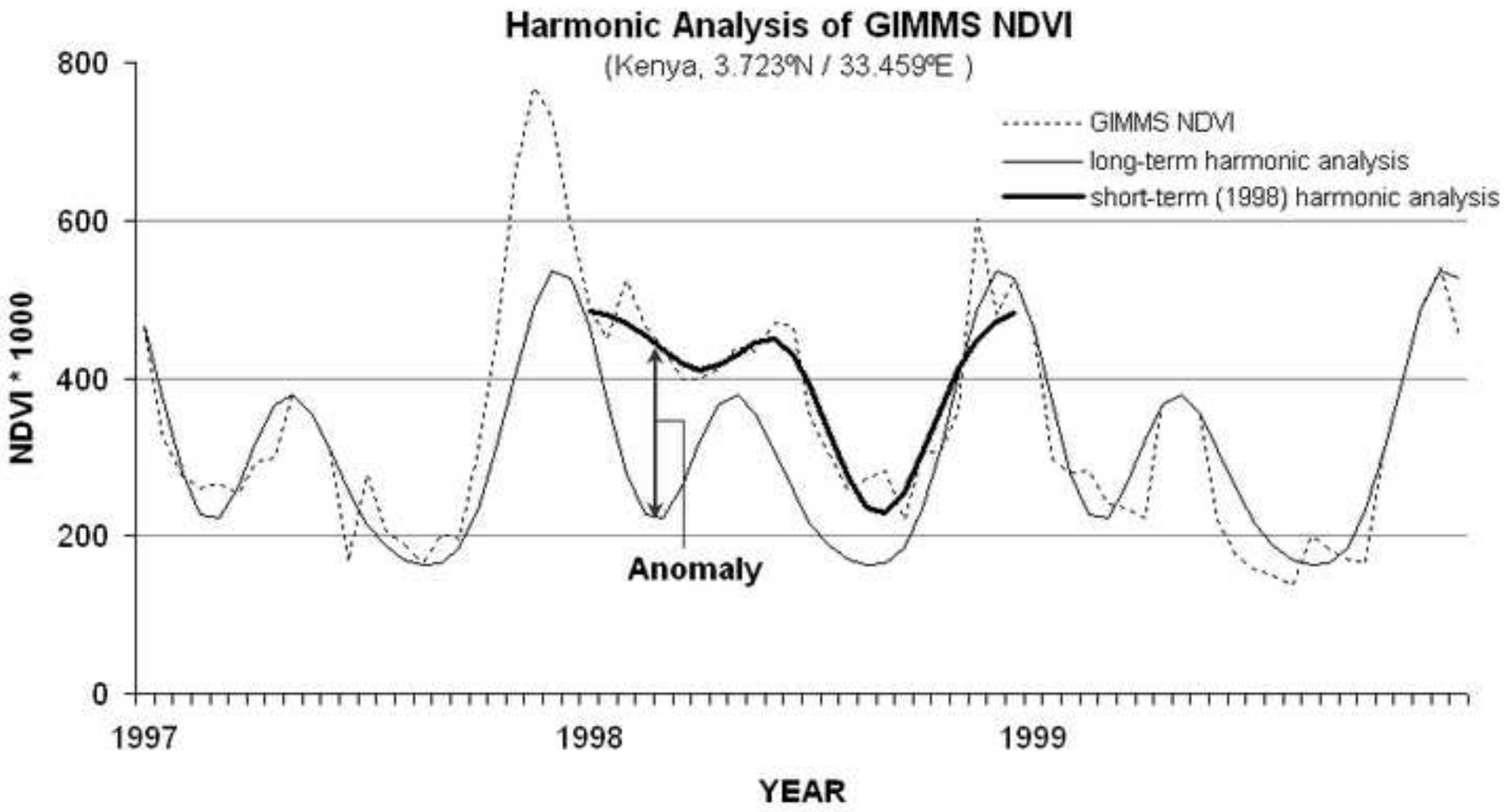

Figure4

Click here to download high resolution image

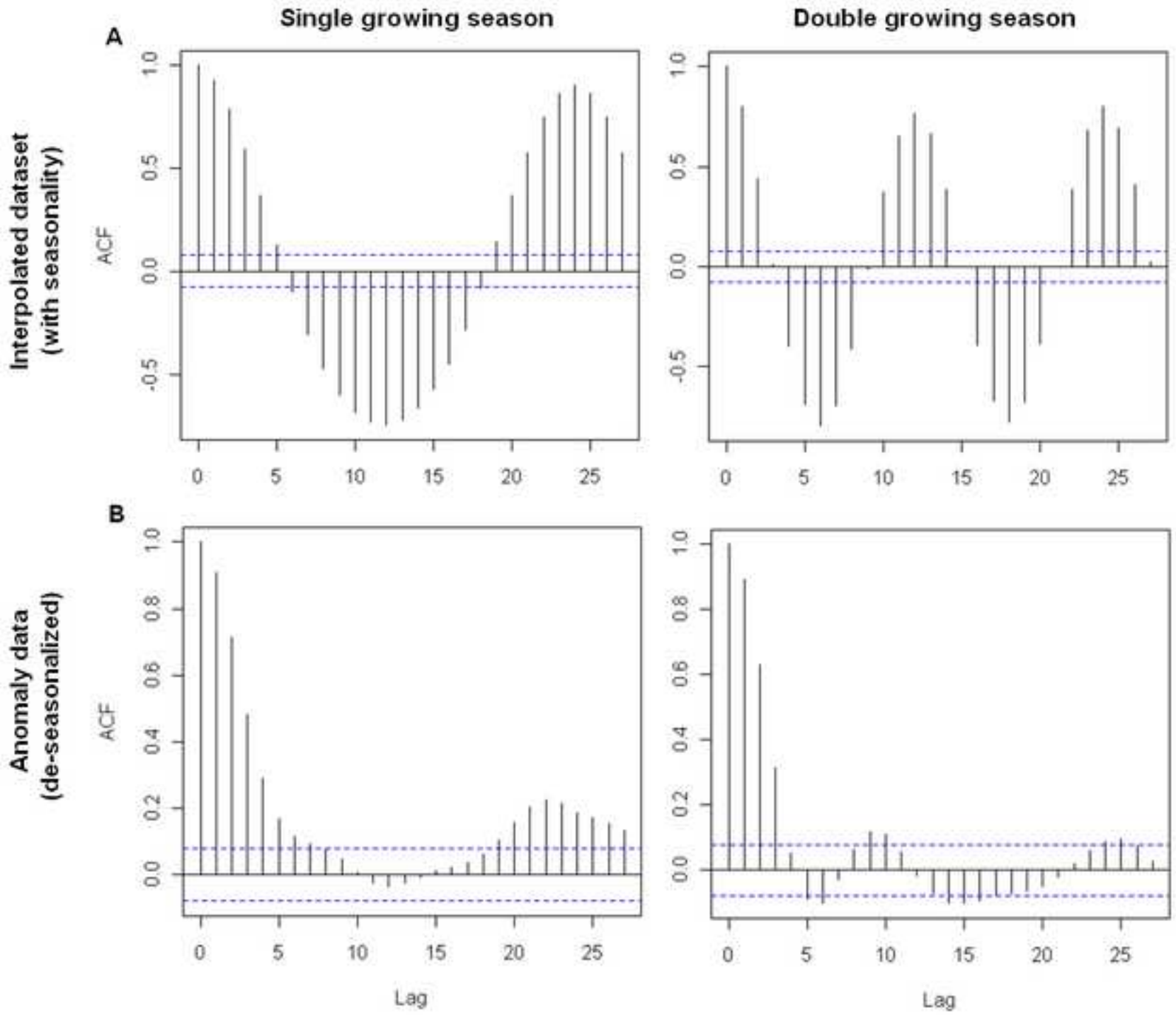

Figure5

Click here to download high resolution image

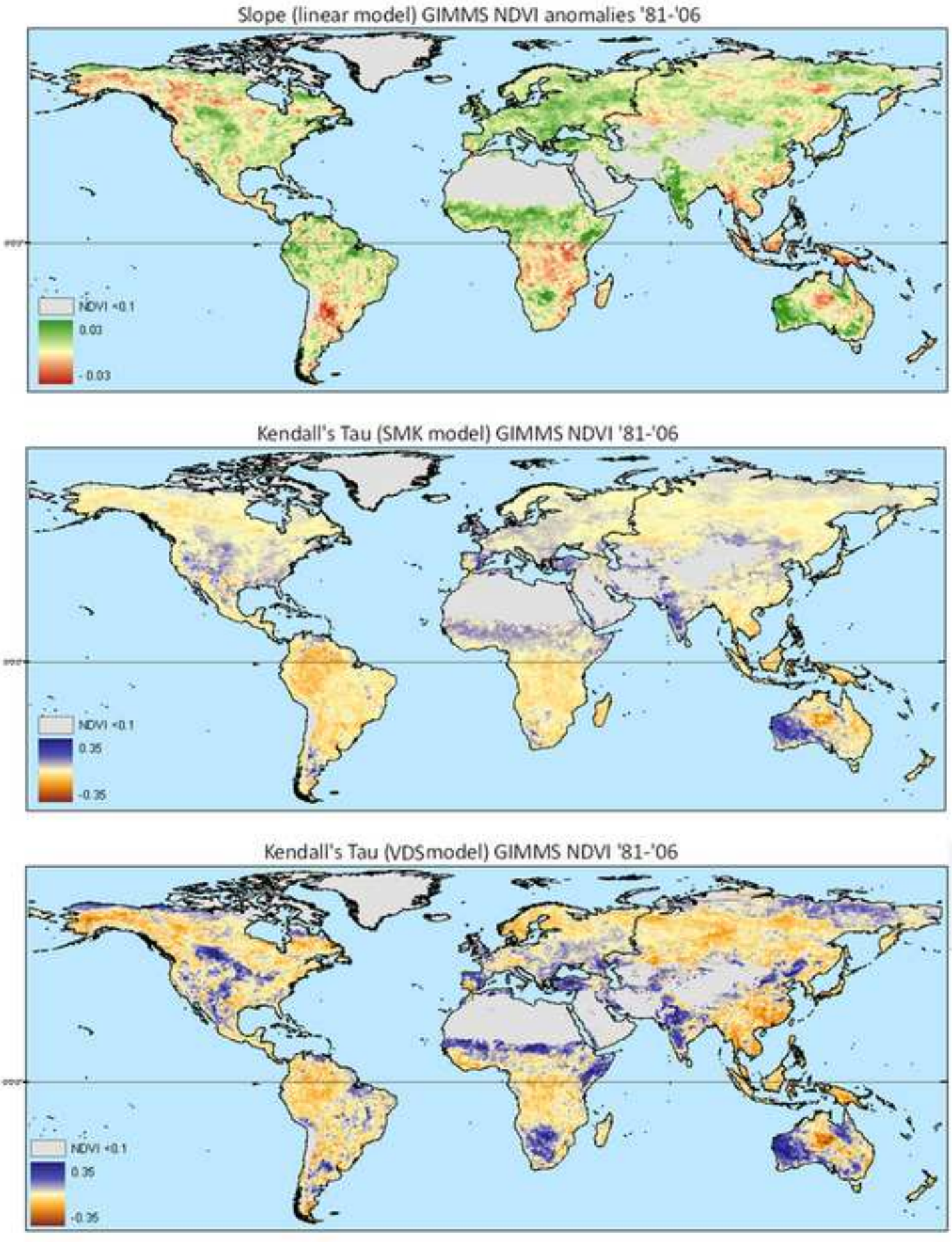

Figure6

Click here to download high resolution image

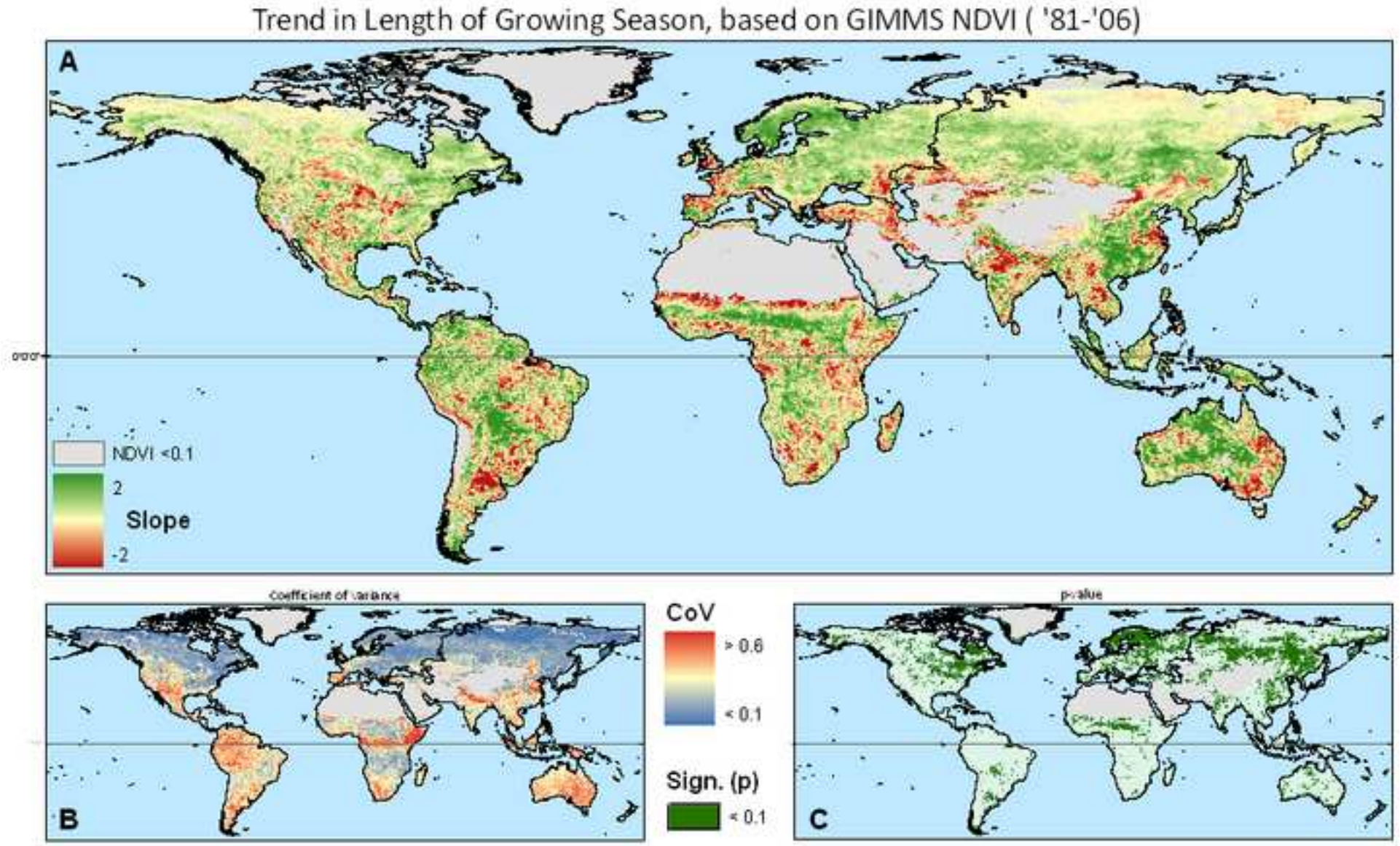

Figure7

Click here to download high resolution image

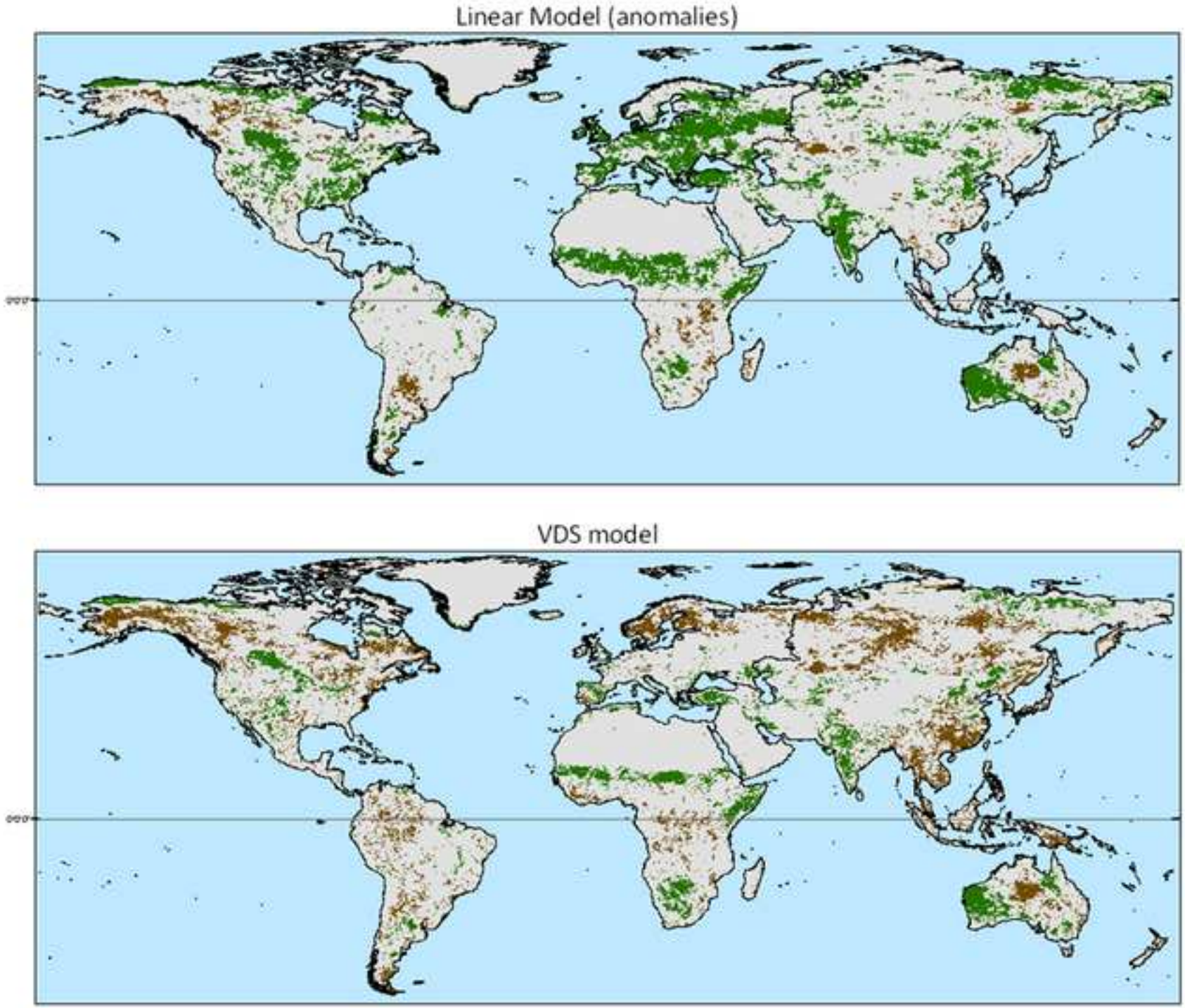

Figure8

Click here to download high resolution image

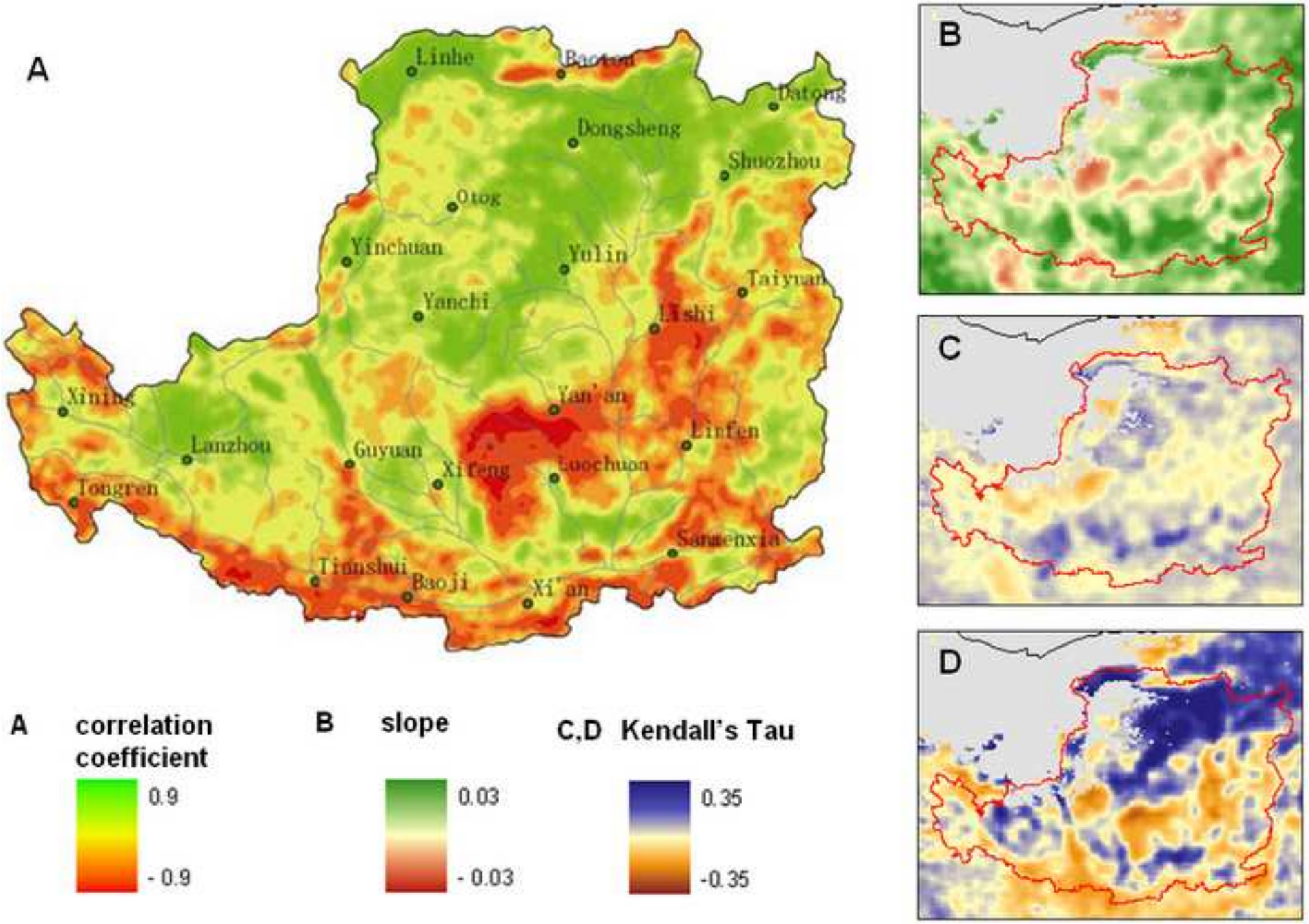

Figure9

Click here to download high resolution image

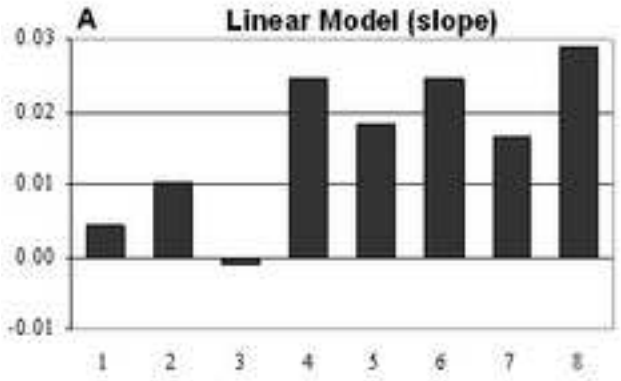

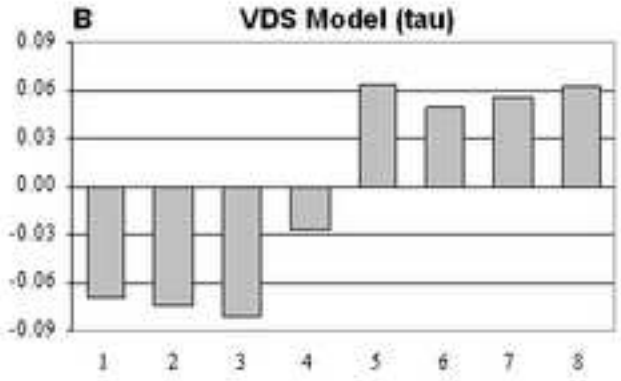

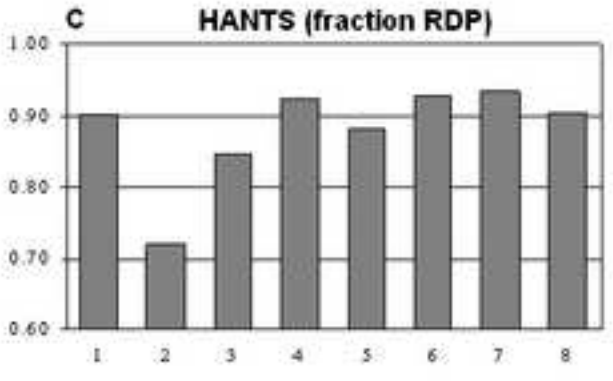

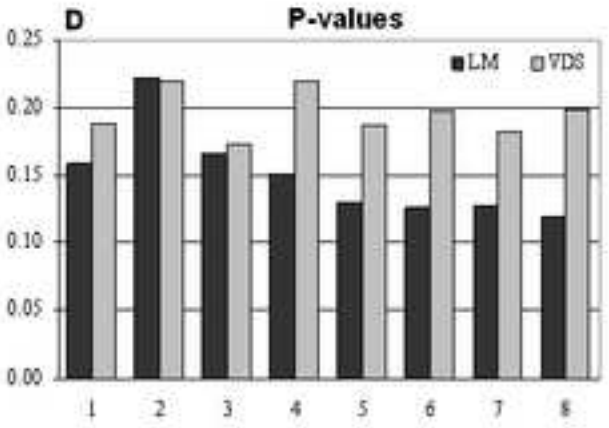

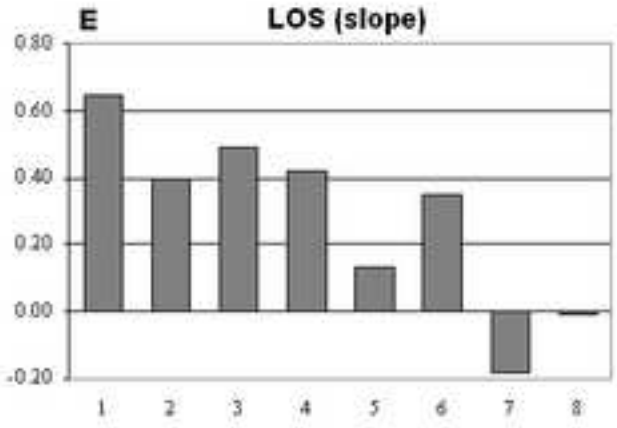

No.	IGBP name	IGBP no.
1	Evergreen Needleleaf Forest	1
2	Evergreen Broadleaf Forest	2
3	Deciduous Needleleaf Forest	3
4	Deciduous Broadleaf / Mixed Forest	4,5
5	Shrublands	6,7
6	(Woody) Savannas	8,9
7	Grasslands	10
8	Croplands	12,14